Bioorganic Chemistry 88 (2019) 102809

Contents lists available at ScienceDirect

Bioorganic Chemistry

journal homepage: www.elsevier.com/locate/bioorg

Hydrazones as novel epigenetic modulators: Correlation between TET 1 protein inhibition activity and their iron(II) binding ability

Milan Jakubek[a,b,c], Zdeněk Kejík[c], Robert Kaplánek[a,b], Veronika Antonyová[a,c], Róbert Hromádka[c,d], Viera Šandriková[d], David Sýkora[b], Pavel Martásek[c,e], Vladimír Král[a,b,c,*]

[a] BIOCEV, First Faculty of Medicine, Charles University, Průmyslová 595, 252 50 Vestec, Czech Republic
[b] Department of Analytical Chemistry, Faculty of Chemical Engineering, University of Chemistry and Technology, Technická 5, 166 28 Prague 6, Czech Republic
[c] Department of Paediatrics and Adolescent Medicine, First Faculty of Medicine, Charles University, Ke Karlovu 2, 121 08 Prague 2, Czech Republic
[d] Research and Development Center C2P s.r.o., Jungmannova 101, 503 51 Chlumec nad Cidlinou, Czech Republic
[e] General University Hospital in Prague, U nemocnice 2, 121 08 Prague 2, Czech Republic

ARTICLE INFO

Keywords:
Epigenetic
Hydrazone
Inhibitor
Iron(II) affinity
TET 1 protein

ABSTRACT

Ten-eleven translocation protein (TET) 1 plays a key role in control of DNA demethylation and thereby of gene expression. Dysregulation of these processes leads to serious pathological states such as oncological and neurodegenerative ones and thus TET 1 targeting is highly requested. Therefore, in this work, we examined the ability of hydrazones (acyl-, aroyl- and heterocyclic hydrazones) to inhibit the TET 1 protein and its mechanism of action. Inhibitory activity of hydrazones **1–7** towards TET 1 was measured. The results showed a high affinity of the tested chelators for iron(II). The study clearly showed a significant correlation between the chelator's affinity for iron(II) ions (represented by the binding constant) and TET 1 protein inhibitory activity (represented by IC_{50} values).

1. Introduction

Epigenetics is a popular topic in the biological sciences, with a high medicinal impact. The epigenetic control of chromatin structure is an important mechanism for the adaptation of gene expression that can depend on external conditions. It is not surprising that epigenetic mechanisms are one of the most important regulation strategies in living systems. Currently, epigenetic drugs are being intensively studied and tested, and initial medicinal applications are underway [1–4]. Most epigenetic drugs suppress the level of DNA methylation and histone acetylation. Their undeniable success has led to the study of the regulation of other epigenetic mechanisms, such as hydroxymethylation of DNA.

A number of recent works have demonstrated that hydroxymethylcytosine, similar to methylcytosine, is important for the regulation of gene expression, but unlike methylcytosine it is associated with its activation [5]. Hydroxymethylcytosine plays an important part in control of the cytoskeleton, ion transport, transcription, cell adhesion, cell death, development, differentiation, maturation, chromatin structure, splicing, self-renewal, myelopoiesis and other key cellular processes. The dysregulation of these processes has serious health consequences and can lead to serious pathological states. Some authors have shown that imbalance in the hydroxymethylcytosine level is associated with the pathogeneses of some serious diseases such as acute myeloid leukaemia [6], RET syndrome [7] and Parkinson's and Alzheimer's disease [8,9], among others. Human tumours also undergo massive changes in DNA methylation [10].

One possible way to modulate the hydroxymethylcytosine level could be based on the regulation of TET 1 protein activity. The TET 1 protein (ten-eleven translocation methylcytosine dioxygenase 1) is an iron(II)- and α-ketoglutarate-dependent dioxygenase and converts 5-methylcytosine to 5-hydroxymethylcytosine. The high importance of the TET 1 protein for the control gene expression has been demonstrated. Due to its importance, studying the mechanisms for controlling TET 1 activity can be a possible route for the development of new therapies. However, this promising strategy is strongly limited by the small number of described effectors of TET 1. One possible method is TET 1 protein inhibition by iron chelators [11]. Alternatively, vitamin C [12] can be used for TET 1 activation, or nickel(II) ions [13] for TET 1 inhibition. This use indicates that the development and study of specific and selective iron(II) chelators for the inhibition of TET protein 1 can have great potential in clinical research and in future medicinal

* Corresponding author at: Department of Paediatrics and Adolescent Medicine, First Faculty of Medicine, Charles University, Ke Karlovu 2, 121 08 Prague 2, Czech Republic.
E-mail address: Vladimir.Kral@lf1cuni.cz (V. Král).

https://doi.org/10.1016/j.bioorg.2019.02.034
Received 15 October 2018; Received in revised form 16 January 2019; Accepted 15 February 2019
Available online 16 February 2019
0045-2068/

applications. In medicinal research, several types of chelators are intensively studied for the treatment of many serious pathological states such as oncological, neurodegenerative and metabolomic diseases [14,15].

The above facts clearly demonstrate the importance for the recognition and strong complexation of iron(II) by chelators. It is well known that the iron(II) cation, with a lower charge density, prefers to interact with binding groups containing 'soft' donor atoms [16]. Structural motifs of known iron(II) chelators are usually based on the nitrogen heteroaromatic groups that act as the binding unit [17–20]. Phonsri et al. showed that the incorporation of aromatic hydroxyl groups in the chelation could be a possible method for the complexation of iron(II) ions [21]. One possible strategy for the construction of chelators that effectively combine both N- and O-metal binding groups is the addition of a hydrazone structural motif in the chelator design. Currently, there are many known hydrazone-based chelators with excellent usability for the complexation of transition metal ions. Depending on the target metal and chosen medium, the binding properties can be finely tuned by their combination with other suitable groups with metal binding affinity, such as benzoisothiazole-1,1-dioxide and pyrimidine, or groups enabling a better solubility (for example, bile acids). Fria et al. successfully tested benzoisothiazole-1,1-dioxide derivatives for the chelation of iron(II) [22]. Another iron(II) chelators based on pyrimidine structure motif were described by Vasta et al. [23,24]. Authors clearly proved, that prepared chelators displayed not only significant inhibition activity of prolyl 4-hydroxylases (iron(II)- and α-ketoglutarate-dependent dioxygenases) via chelation of iron(II). For some of them it was found selective mod of inhibition caused by their incorporation to enzyme active site. Combination of 2-hydroxyaryl or 2-*N*-heteroaryl moiety with benzoisothiazole-1,1-dioxide via suitable linker such as hydrazone can be promising way for the preparation of new iron(II) chelator. Another important part of chelator design is optimization of their solubility and hydrophilicity. Incorporation of bile acid structural motif into hydrazone-type chelators can improve their solubility in aqueous medium and their bioavailability. In the present time, cholic acid is used for the tuning chelator properties, especially ones for medicinal and biological applications [25–27]. Therefore, in this work, we designed, prepared and studied hydrazones containing a benzoisothiazole-1,1-dioxide or cholic acid moiety as a novel class of potential TET 1 protein inhibitors.

2. Results and discussion

2.1. Chemistry

All of the chelators were based on hydrazones. Chelators **1–4** represent hydrazones derived from 2-*N*-heterocyclic hydrazine, and they possess an N—N—O or N—N—N chelating unit. Chelators **5** and **6** represent hydrazones of aliphatic carbohydrazide, and chelator **7** represents a hydrazone of aroylhydrazide. Chelators **5–7** possess O—N—O or O—N—N chelating units (Fig. 1).

Chelators **1–7** were prepared by the reaction of corresponding hydrazine derivatives with substituted salicylaldehydes or 2-*N*-heteroaromatic aldehydes and methylketones. Thus, chelators **1–4** were prepared by reaction of 3-hydrazinylbenzoisothiazole-1,1-dioxide [28] with excess of carbonyl compound (5-nitro-2-hydroxybenzaldehyde for **1**, 2,3-dihydroxybenzaldehyde for **2**, pyridine-2-carboxaldehyde for **3** and acetylpyrazine for **4**) in isopropanol in the presence of acetic acid at 75 °C for 48 h, with yields of 78–95% (Scheme 1). Chelators **5** and **6** were prepared according to the literature [15] by reaction of cholic hydrazide with 2-hydroxy-3-methoxybenzaldehyde and quinoline-2-carboxaldehyde, respectively (Scheme 2). Chelator **7** was prepared according to the literature [15] by reaction of 4-(cholylamido)benzhydrazide with 2-hydroxy-3-methoxybenzaldehyde (Scheme 2).

2.1.1. Prototropic tautomerism of chelators 1–4

In some cases, heterocyclic hydrazones showed prototropic tautomerism—equilibrium between the amino form (acidic proton is on the hydrazine nitrogen) and the imino form (acidic proton is on the heterocyclic nitrogen) (Scheme 3) [28,29]. Prototropic tautomerism leads to two sets of signals in the ^{1}H and ^{13}C NMR spectra.

2.2. Chelation ability towards iron(II) ions

Because the anticipated inhibition model of TET 1 protein by the tested compound is based on the complexation of iron(II) ions, the compound's chelation ability for iron(II) ions in water was investigated by UV–Vis spectroscopy. The determined value of the binding constant is shown in Table 1. The affinity was found for chelator **1**. On the other hand, chelator **3** and **4** showed no significant interaction with iron(II) ions; this implies the importance of the aromatic hydroxyl of the chelator for the complexation of iron(II) ions. The reason for chelator **1** displaying significantly higher affinity than chelator **2** can be explained by the reduction of electron density in the phenyl group, and therefore the hydroxyl group, by the electron acceptor nitro group. This phenomenon leads to the strong dissociation of hydroxy groups, thereby supporting chelation. Additionally, in the case of cholic chelators **5**, **6** and **7**, the value of their binding constant showed the positive influence of the aromatic hydroxyl groups on their chelation ability (Fig. 2 and Table 1).

2.3. Inhibition of TET 1 protein

The usability of the tested chelators for the inhibition of TET 1 was determined by a fluorometric TET hydroxylase activity quantification kit. The best inhibitory effect was observed for chelator **1**. The dependence of TET 1 activity on its concentration is shown in Fig. 3. The inhibitory activity of chelators **1–7** (as IC_{50} values) is summarized in Table 2. The lowest IC_{50} value was determined for chelator **1**, the compound with the highest affinity for iron(II) ions, indicating that the inhibition mechanism is based on the chelation of iron(II) (which is a cofactor of the TET 1 protein). In accordance with this hypothesis, we observed a significant correlation between the affinity of tested chelators **1–7** for iron(II) and their inhibition activity. In addition, chelators **3**, **4** and **6**, with low or no affinity for iron(II) ions, displayed no significant inhibition activity. The obtained results implied that the observed inhibition of TET 1 could be based on the chelation of iron(II) ions. More importantly, obtained data strongly implied that mechanism of inhibition of tested chelators is not only based on nonselective complexation free iron(II). For example, corresponding concentration of tested chelators for IC_{50} caused reduction of enzyme activity to the half, but maximal amount of chelated iron(II) was significantly lower (Table 2). It indicates possibility of new inhibition mode. Most probably, tested chelators form complex with iron(II) ion in the active site of TET 1 protein. Similar phenomenon was described by Vasta et al., which studied inhibition prolyl 4-hydroxylases (iron(II)- and α-ketoglutarate-dependent dioxygenase) by iron(II) chelators. [23,24] It implies that inhibition effect of some tested chelators, especially chelator **1** could be based on the specific targeting of TET 1 protein.

2.4. In silico prediction of LD_{50} values

It should be mentioned that hydrazone-based chelators could possess potential toxicity, which could be complicated their possible applications [30]. Therefore we used online ProTox-II program [31] for the prediction of LD_{50} values. *In silico* ADME predictions showed very low toxicity of tested compounds, LD_{50} values for chelators **1–7** are in the range of 1.0–14.2 g/kg (see you in the Table 3). Fact that, determined IC_{50} value of tested chelator **1–7** was micromolar and submicromolar, indicated promising applicability of hydrazine chelators as TET 1 inhibitor.

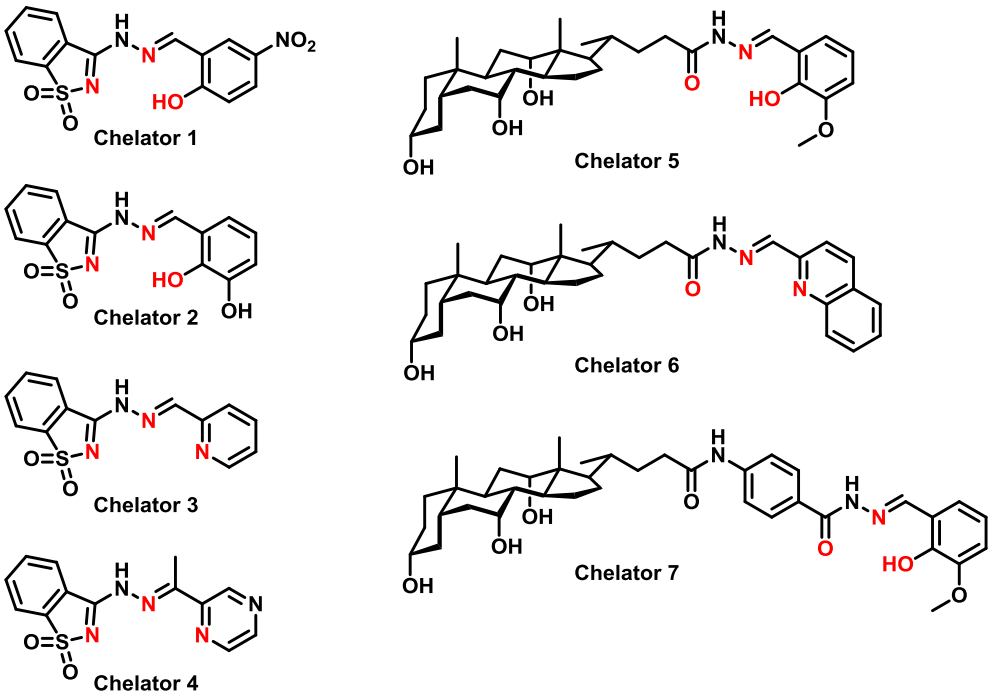

Fig. 1. Structures of hydrazones **1–7** with highlighted chelating system.

3. Conclusions

Epigenetic drugs may induce alterations in DNA methylation patterns by inhibition of the TET 1 protein, which is a key enzyme for the oxidation of 5-methylcytosine to 5-hydroxymethylcytosine. In the present work, a series of heterocyclic, acyl- and aroylhydrazones (chelators) was designed, prepared and tested as potential epigenetically active compounds for the modulation (inhibition) of the TET 1 protein. Binding abilities of the studied chelators **1–7** towards iron(II) ions were evaluated using UV–Vis absorption spectroscopy. Their inhibition activity was determined by a fluorometric TET hydroxylase activity quantification kit. The results of these studies proved the existence of a significant correlation between the affinity of hydrazone for iron(II) ions and the inhibitory activity towards TET 1 and showed the great potential of hydrazones as a novel class of epigenetic modulators.

In the future, we plan to focus on *in vitro* study of TET 1 inhibitors based on novel hydrazone-based chelators. Detailed determination of mechanism of inhibition will be also studied.

4. Experimental section

4.1. Materials and methods

All chemicals and solvents were purchased from Sigma–Aldrich (Czech Republic) and were used without further purification. The recombinant TET 1 protein and TET hydroxylase activity fluorometric quantification kits were obtained from Active Motif (USA) and Abcam (UK), respectively. The UV–Vis absorption spectra were recorded using a Varian Cary 400 SCAN UV–Vis spectrophotometer (Varian, USA) where the reference spectrum of plain solvent was subtracted from all sample spectra. The NMR spectra were obtained with a Bruker Avance III 500 MHz (500 MHz for ^{1}H and 125 MHz for ^{13}C) (Bruker, Germany) at 25 °C in DMSO-d_6. The chemical shifts (δ) are presented in ppm (relative to TMS = 0.000 ppm), and the coupling constants (J) are presented in Hz. Mass spectra were measured with a 3200 Q TRAP (AB Sciex, Canada) mass spectrometer fitted with an electrospray ion source. The analytes dissolved in methanol were introduced directly into the ESI source via a PEEK capillary at a flow rate of 10 µL/min. Nitrogen was used as a nebulizer gas. The operating conditions for the mass spectrometer were set as follows: ion spray voltage 5.5 kV; curtain gas 10; ion source gas(1) 18 psig; ion source gas(2) 0 psig; ion source temperature ambient; declustering potential 60 V; and entrance potential 10 V.

4.2. Synthesis and characterization of chelators

4.2.1. Chelator *1*

The synthesis and characterization of chelator **1** is described in detail elsewhere [29]. 3-Hydrazinylbenzoisothiazole-1,1-dioxide [28] (138 mg; 0.7 mmol) and 2-hydroxy-5-nitrobenzaldehyde (167 mg;

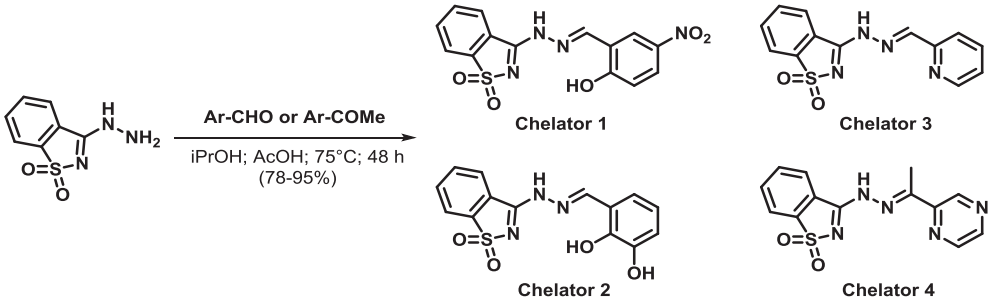

Scheme 1. Preparation of chelators **1–4**.

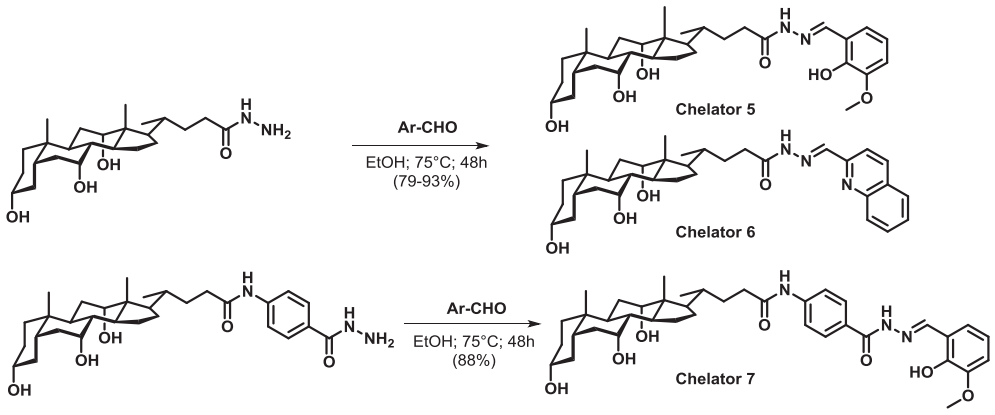

Scheme 2. Preparation of chelators **5–7**.

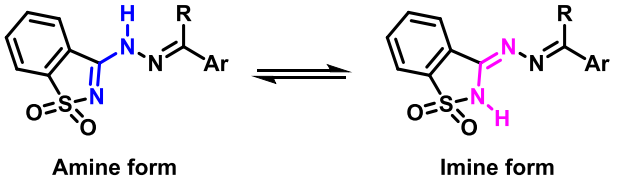

Scheme 3. Prototropic tautomerism of chelators **1–4**.

Table 1
Value of binding constants and complex stoichiometry of chelators **1–7** with iron(II) ions.

Chelator	Log(K)	St[a]
1	6.8	1:1
	15	1:2
2	7.3	1:1
	14	1:2
3	–	–
4	–	–
5	3.8	1:1
6	3.3	1:1
7	3.8	1:1

[a] Stoichiometry (iron(II) ions:Chelator).

1 mmol) were mixed in isopropanol (25 mL), and acetic acid (1 mL) was added. The reaction mixture was stirred at 75 °C for 2 days. The volatile compounds were then evaporated under reduced pressure, and the residue was suspended in a diethyl ether/petroleum ether mixture (1:1, v/v; 30 mL). Solid material was filtered, washed with additional diethyl ether/petroleum ether mixture (1:1, v/v; 60 mL) and dried at 50 °C

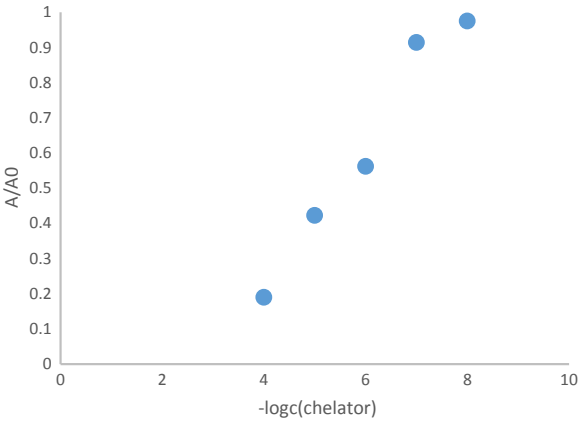

Fig. 3. Dependence of normalised TET 1 activity (enzyme activity in the presence of chelator/activity of non-inhibited enzyme) on the concentration of chelator **1**.

Table 2
IC_{50} values for chelators **1–7** for TET 1 and amount of chelated iron(II).

Chelator	IC_{50} (μM)	Chelated Fe(II) (%)
1	0.79	0.7
2	9.1	9.1
3	–	–
4	–	–
5	8.0	8.0
6	–	–
7	15	15

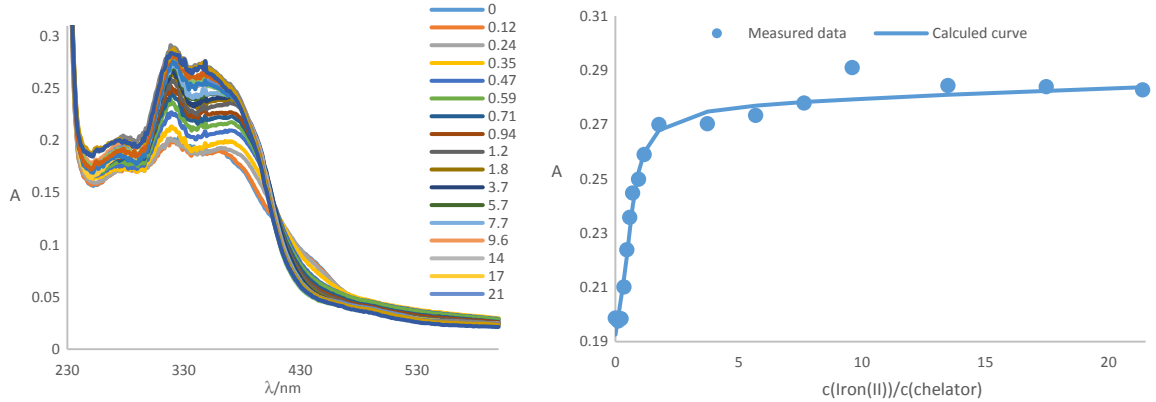

Fig. 2. UV–Vis spectra of chelator **1** in the presence of iron(II) ions (A) and titration curve (B) for chelator **1** (10 μM) showing the dependence of the complex absorbance at 321 nm on the iron(II) concentration in aqueous medium (water/DMSO, 99:1, v/v).

Table 3
Predicted LD_{50} values for chelators **1–7**.

Chelator	LD_{50} (g/kg)
1	4.5
2	14.2
3	2.0
4	2.0
5	1.0
6	1.4
7	4.5

under vacuum. 2-((2-(1,1-Dioxidobenzoisothiazol-3-yl)hydrazinylidene)methyl)-4-nitrophenol (**1**) was obtained with a yield of 240 mg (92%) as a yellowish solid.

4.2.2. Chelator *2*

3-Hydrazinylbenzoisothiazole-1,1-dioxide (138 mg; 0.7 mmol) and 2,3-dihydroxybenzaldehyde (138 mg; 1 mmol) were mixed in isopropanol (25 mL), and acetic acid (1 mL) was added. The reaction mixture was then stirred at 75 °C for 2 days. The volatile compounds were then evaporated under reduced pressure, and the residue was suspended in a diethyl ether/petroleum ether mixture (1:1, v/v; 30 mL). Solid material was filtered, washed with additional diethyl ether/petroleum ether mixture (1:1, v/v; 60 mL) and dried at 50 °C under vacuum. 3-((2-(1,1-Dioxido-1,2-benzothiazol-3-yl)hydrazinylidene)methyl)benzene-1,2-diol (**2**) was obtained with a yield of 212 mg (95%) as a white solid. ^{1}H NMR (DMSO-d_6): δ 6.77 (m, 1H); 6.92 (dd, J = 7.9, 1.5 Hz, 1H); 7.19 and 7.32 (2x dd, J = 7.9, 1.5 Hz, 1H); 7.90 (m, 2H); 8.07 (m, 1H), 8.24 and 8.69 (m, 1H); 8.83 (s, 1H); 9.27 and 9.56 (2x s, 1H); 9.82 and 10.28 (2x s, 1H); 12.71 and 13.00 (2x bs, 1H) ppm. ^{13}C NMR (DMSO-d_6): δ 116.3 (117.3); 118.1 (118.9); 118.9 (120.2); 119.4 (119.5); 121.7 (121.5); 123.3 (129.5); 126.6 (126.7); 133.3 (133.5); 133.8 (134.0); 141.9 (143.3); 145.8 (145.9); 146.5 (146.0); 151.5 (147.4); 155.7 (158.5) ppm. ESI-MS (m/z): 318 $[M+H]^+$. Elem. Anal. Calcd. for $C_{14}H_{11}N_3O_4S$: C, 52.99; H, 3.49; N, 13.24. Found: C, 52.96; H, 3.53; N, 13.22.

4.2.3. Chelator *3*

3-Hydrazinylbenzoisothiazole-1,1-dioxide (138 mg; 0.7 mmol) and pyridine-2-carbaldehyde (107 mg; 1 mmol) were mixed in isopropanol (25 mL), and acetic acid (1 mL) was added. The reaction mixture was then stirred at 75 °C for 2 days. The volatile compounds were then evaporated under reduced pressure, and the residue was suspended in diethyl ether/petroleum ether mixture (1:1, v/v; 30 mL). Solid material was filtered, washed with additional diethyl ether/petroleum ether mixture (1:1, v/v; 60 mL) and dried at 50 °C under vacuum. 3-[2-(Pyridin-2-ylmethylidene)hydrazinyl]-1,2-benzothiazole 1,1-dioxide (**3**) was obtained with a yield of 184 mg (92%) as a white solid. ^{1}H NMR (DMSO-d_6): δ 7.50 (m, 1H); 7.92 (m, 3H); 8.08 (m, 2H); 8.26 and 8.83 (2x m, 1H); 8.38 and 8.60 (2x s, 1H); 8.70 (m, 1H); 12.68 and 13.22 (2x bs, 1H) ppm. ^{13}C NMR (DMSO-d_6): δ 120.9 (121.0); (121.7) 121.8; 123.4 (129.6); (125.2) 125.4; (126.4) 126.7; 133.4 (133.8); 134.0 (134.3); 137.2 (137.3); 141.7 (143.1); 149.9 (150.0); (151.9) 152.1; (150.6) 152.4; 156.3 (159.1) ppm. ESI-MS (m/z): 287 $[M+H]^+$. Elem. Anal. Calcd. for $C_{13}H_{10}N_4O_2S$: C, 54.54; H, 3.52; N, 19.57. Found: C, 54.51; H, 3.54; N, 19.56.

4.2.4. Chelator *4*

3-Hydrazinylbenzoisothiazole-1,1-dioxide (138 mg; 0.7 mmol) and acetylpyrazine (122 mg; 1 mmol) were mixed in isopropanol (25 mL), and acetic acid (1 mL) was added. The reaction mixture was then stirred at 75 °C for 2 days. The volatile compounds were then evaporated under reduced pressure, and the residue was suspended in diethyl ether/petroleum ether mixture (1:1, v/v; 30 mL). Solid material was filtered, washed with additional diethyl ether/petroleum ether mixture (1:1, v/v; 60 mL) and dried at 50 °C under vacuum. 3-(2-(1-(Pyrazin-2- yl) ethylidene)hydrazinyl)-1,2-benzothiazole 1,1-dioxide (**4**) was obtained with a yield of 164 mg (78%) as a yellowish solid. ^{1}H NMR (DMSO-d_6): 2.55 and 2.61 (2x s, 3H); 7.92 (m, 2H); 8.10 (s, 1H); 8.45 and 8.70 (2x m, 1H); 8.75 (m, 2H); 9.30 (s, 1H); 11.70 and 12.37 (2x bs, 1H) ppm. ^{13}C NMR (DMSO-d_6): δ 12.8 (13.6); 121.7 (121.6); 124.2; 126.7; 129.6; 133.8 (134.1); 133.9; 142.5; 143.0; 143.6 (143.8); 145.3 (145.0); 149.8 (149.7); 154.7 (159.9) ppm. ESI-MS (m/z): 302 $[M+H]^+$. Elem. Anal. Calcd. for $C_{13}H_{11}N_5O_2S$: C, 51.82; H, 3.68; N, 23.24. Found: C, 51.80; H, 3.72; N, 23.26.

4.2.5. Chelator *5*

The synthesis and characterization of chelator **5** is described in detail elsewhere [15]. Cholyl hydrazide (169 mg; 0.4 mmol) and 2-hydroxy-3-methoxybenzaldehyde (67 mg; 0.44 mmol) were mixed in ethanol (40 mL) and heated to 75 °C for 48 h. The volatile compounds were then removed under reduced pressure, and the residue was triturated with diethyl ether (40 mL). The solid product was filtered off and washed with additional diethyl ether (40 mL) and dried under vacuum at 50 °C. *N*'-(2-hydroxy-3-methoxybenzylidene)cholylhydrazide (**5**) was obtained with a yield of 207 mg (93%) as a white solid.

4.2.6. Chelator *6*

The synthesis and characterization of chelator **6** is described in detail elsewhere [15]. Cholyl hydrazide (169 mg; 0.4 mmol) and quinoline-2-carbaldehyde (69 mg; 0.44 mmol) were mixed in ethanol (40 mL) and heated to 75 °C for 48 h. The volatile compounds were then removed under reduced pressure, and the residue was triturated with diethyl ether/petroleum ether mixture (1:1, v/v; 40 mL). The solid product was filtered off and washed with additional diethyl ether/petroleum ether mixture (1:1, v/v; 40 mL) and dried under vacuum at 50 °C. *N*'-(quinolin-2-ylmethylene)cholylhydrazide (**6**) was obtained with a yield of 177 mg (79%) as an off-white solid.

4.2.7. Chelator *7*

The synthesis and characterization of chelator **7** is described in detail elsewhere [15]. 4-(Cholylamido)benzhydrazide (87 mg; 0.16 mmol) and 2-hydroxy-3-methoxybenzaldehyde (49 mg; 0.32 mmol) were mixed in ethanol (20 mL) and heated to 75 °C for 48 h. The volatile compounds were then removed under reduced pressure, and the residue was triturated with diethyl ether/petroleum ether mixture (1:1, v/v; 20 mL). The solid product was filtered off and washed with additional diethyl ether/petroleum ether mixture (1:1, v/v; 30 mL) and dried under vacuum at 50 °C. *N*'-(2-hydroxy-3-methoxybenzylidene)-4-(cholylamido)benzhydrazide (**7**) was obtained with a yield of 95 mg (88%) as a white solid.

4.3. Determination of conditional binding constants and complex stoichiometry of chelators *1–7* with iron(II) ions

The association of chelators **1–7** with iron(II) ions was studied using UV–Vis spectroscopy in aqueous solution (water/DMSO, 99:1, v/v). Because the solvent always significantly affects the binding constants, all titrations were performed in the same environment, and the ratio of DMSO to water was held constant. Conditional constants (Ks) were calculated from the absorbance changes ΔA of chelators **1–7** at the spectral maximum of their complexes with iron(II) by nonlinear regression analysis with the Letagrop Spefo 2005 software. The computational model is described and discussed in detail elsewhere [32].

The concentration of chelators **1–7** was 10 μM. The concentrations of iron(II) varied in the range of 0–0.5 mM. UV–Vis spectra were measured from 220 to 900 nm, with 1-nm data spacing in a 1-cm quartz cell at a scan rate of 600 nm/min.

4.4. IC_{50} determination of chelators **1–7** for the TET 1 protein

The activity of TET 1 protein was determined using the Abcam TET Hydroxylase Activity Quantification Kit (Fluorometric). A 96-well microtiter plate was activated according to the manual (application of binding solution and TET substrate). Calculated amounts of the tested chelators were dissolved in DMSO to obtain a concentration of 0.01 M in a 1 mL volumetric flask. A total of 25 μg of TET 1 protein was diluted in TET 1 assay buffer in a 5 mL volumetric flask. Concentration of ascorbic acid, α-ketoglutarate and ferric sulphate in diluted TET assay buffer were 2, 1 and 0.1 mmol/l, respectively. A DMSO solution of the chelator was subsequently diluted with the TET assay buffer to the chelator concentrations of 10^{-7}, 10^{-6}, 10^{-5}, 10^{-4}, and 10^{-3} mol/L with 10% DMSO in a 1 mL volumetric flask. Subsequently, 50 μL of the final TET assay buffer was applied, with the addition of TET 1 protein and 5 μL of chelator solution, into the prepared microarrays. In the case of control experiments (TET 1 alone without inhibitors), 5 μL of final TET assay buffer with 10% DMSO was used. The tested chelator concentrations were 10^{-8} 10^{-7}, 10^{-6}, 10^{-5}, 10^{-4} and 0 mol/L. The subsequent steps of the kit were carried out according to the manual. In the next step, wells were washed by wash-buffer and capture antibody was applied. In the subsequent step, wells were washed by wash-buffer and detection antibody and then enhancer solution was used. After application of the fluorescence development kit, fluorescence was measured at 590 nm (λ_{ex} = 530 nm) and was used to calculate the residual activity of TET 1. For active chelators, the IC_{50} values were determined.

4.5. Toxicity prediction

On the basis of structural models, drawn in ChemDraw software (Cambridge Software), ADME toxicity of tested chelators **1–7** (represent LD_{50} value) were calculated using online ProTox-II program [31].

Disclosure statement

No potential conflicts of interest were reported by the authors.

Acknowledgements

This work was supported by the Ministry of Education, Youth and Sports of the Czech Republic within the National Sustainability Program II [Project BIOCEV-FAR, LQ1604] and by the project "BIOCEV" [CZ.1.05/1.1.00/02.0109]; the Technology Agency of the Czech Republic [project TE01020028]; Ministry of Industry and Trade within project [FV20572]; Ministry of Agriculture of the Czech Republic [QJ1610515], Charles University in Prague [UNCE 204064, SVV 260 364 and PROGRES Q26/LF1]. This work was also supported by the "Operational Programme Prague – Competitiveness" (CZ.07.1.02/0.0/0.0/16_040/0000376) and the "National Programme of Sustainability I" - NPU I (LO1601 - No. MSMT-43760/2015). Additionally, we thank the Ministry of Education, Youth and Sports of the Czech Republic grant no. LM201564 (EATRIS-CZ) and Grant Agency of the Czech Republic, grant no. 17-02448S for the financial support of this work.

References

[1] R. Cacabelos, Pharmacogenomics of Alzheimer's and Parkinson's diseases, Neurosci. Lett. (2018), https://doi.org/10.1016/j.neulet.2018.1009.1018.
[2] L. Sommese, G. Benincasa, M. Lanza, A. Sorriento, C. Schiano, R. Lucchese, R. Alfano, G.F. Nicoletti, C. Napoli, Novel epigenetic-sensitive clinical challenges both in type 1 and type 2 diabetes, J. Diabetes Compl. 32 (2018) 1076–1084.
[3] M.J. Hadden, A. Advani, Histone deacetylase inhibitors and diabetic kidney disease, Int. J. Mol. Sci. 19 (2018) 2630.
[4] Z. Kejik, M. Jakubek, R. Kaplanek, J. Kralova, I. Mikula, P. Martasek, V. Kral, Epigenetic agents in combined anticancer therapy, Future Med. Chem. 10 (2018) 1113–1130.
[5] D.Q. Shi, I. Ali, J. Tang, W.C. Yang, New Insights into 5hmC DNA modification: generation, distribution and function, Front. Genet. 8 (2017) Article 100.
[6] H. Huang, X. Jiang, Z. Li, Y. Li, C.X. Song, C. He, M. Sun, P. Chen, S. Gurbuxani, J. Wang, G.M. Hong, A.G. Elkahloun, S. Arnovitz, J. Wang, K. Szulwach, L. Lin, C. Street, M. Wunderlich, M. Dawlaty, M.B. Neilly, R. Jaenisch, F.C. Yang, J.C. Mulloy, P. Jin, P.P. Liu, J.D. Rowley, M. Xu, C. He, J. Chen, TET1 plays an essential oncogenic role in MLL-rearranged leukemia, Proc. Natl. Acad. Sci. U.S.A. 110 (2013) 11994–11999.
[7] T.L. Cheng, J. Chen, H. Wan, B. Tang, W. Tian, L. Liao, Z. Qiu, Regulation of mRNA splicing by MeCP2 via epigenetic modifications in the brain, Sci. Rep. 7 (2017) 42790.
[8] E.M. Ellison, E.L. Abner, M.A. Lovell, Multiregional analysis of global 5-methylcytosine and 5-hydroxymethylcytosine throughout the progression of Alzheimer's disease, J. Neurochem. 140 (2017) 383–394.
[9] J. Zhao, Y. Zhu, J. Yang, L. Li, H. Wu, P.L. De Jager, P. Jin, D.A. Bennett, A genome-wide profiling of brain DNA hydroxymethylation in Alzheimer's disease, Alzheimers Dement. 13 (2017) 674–688.
[10] Y. Liang, P. Xu, Q. Zou, H. Luo, W. Yu, An epigenetic perspective on tumorigenesis: Loss of cell identity, enhancer switching, and NamiRNA network, Semin. Cancer Biol. (2018), https://doi.org/10.1016/j.semcancer.2018.1009.1001.
[11] S. Badal, Y.F. Her, L.J. Maher 3rd, Nonantibiotic effects of fluoroquinolones in mammalian cells, J. Biol. Chem. 290 (2015) 22287–22297.
[12] K. Blaschke, K.T. Ebata, M.M. Karimi, J.A. Zepeda-Martinez, P. Goyal, S. Mahapatra, A. Tam, D.J. Laird, M. Hirst, A. Rao, M.C. Lorincz, M. Ramalho-Santos, Vitamin C induces Tet-dependent DNA demethylation and a blastocyst-like state in ES cells, Nature 500 (2013) 222–226.
[13] R. Yin, J. Mo, J. Dai, H. Wang, Nickel(II) inhibits tet-mediated 5-methylcytosine oxidation by high affinity displacement of the cofactor iron(II), ACS Chem. Biol. 12 (2017) 1494–1498.
[14] R. Kaplanek, M. Jakubek, J. Rak, Z. Kejik, M. Havlik, B. Dolensky, I. Frydrych, M. Hajduch, M. Kolar, K. Bogdanova, J. Kralova, P. Dzubak, V. Kral, Caffeine-hydrazones as anticancer agents with pronounced selectivity toward T-lymphoblastic leukaemia cells, Bioorg. Chem. 60 (2015) 19–29.
[15] C.W. D'Acunto, R. Kaplanek, H. Gbelcova, Z. Kejik, T. Briza, L. Vasina, M. Havlik, T. Ruml, V. Kral, Metallomics for Alzheimer's disease treatment: Use of new generation of chelators combining metal-cation binding and transport properties, Eur. J. Med. Chem. 150 (2018) 140–155.
[16] T. Zhou, Y. Ma, X. Kong, R.C. Hider, Design of iron chelators with therapeutic application, Dalton Trans. 41 (2012) 6371–6389.
[17] D. Tsugama, S.K. Liu, T. Takano, Evaluation of Fe(III) reduction by mitochondria induced with a respiratory substrate NADH or succinate, using a Fe(II)-specific chelator bathophenanthroline disulfonate in Saccharomyces cerevisiae, Biologia 64 (2009) 877–880.
[18] M.T. Stauffer, L.J. Hunter, S.K. Troncone, Determination of iron in abandoned mine drainage by UV-Vis spectrophotometry and flame atomic absorption spectrophotometry, Spectr. Lett. 40 (2007) 429–437.
[19] M. Hamada-Kanazawa, M. Kouda, A. Odani, K. Matsuyama, K. Kanazawa, T. Hasegawa, M. Narahara, M. Miyake, beta-Citryl-L-glutamate is an endogenous iron chelator that occurs naturally in the developing brain, Biol. Pharm. Bull. 33 (2010) 729–737.
[20] G. Park, F.H. Lu, N. Ye, M.W. Brechbiel, S.V. Torti, F.M. Torti, R.P. Planalp, Novel iron complexes and chelators based on cis, cis-1,3,5-triaminocyclohexane: iron-mediated ligand oxidation and biochemical properties, J. Biol. Inorg. Chem. 3 (1998) 449–457.
[21] W. Phonsri, D.S. Macedo, K.R. Vignesh, G. Rajaraman, C.G. Davies, G.N.L. Jameson, B. Moubaraki, J.S. Ward, P.E. Kruger, G. Chastanet, K.S. Murray, Halogen substitution effects on N2O schiff base ligands in unprecedented abrupt Fe(II) spin crossover complexes, Chem.-Eur. J. 23 (2017) 7052–7065.
[22] L.M.T. Frija, R. Fausto, R.M.S. Loureiro, M.L.S. Cristiano, Synthesis and structure of novel benzisothiazole-tetrazolyl derivatives for potential application as nitrogen ligands, J. Mol. Catal. A 305 (2009) 142–146.
[23] J.D. Vasta, R.T. Raines, Selective inhibition of prolyl 4-hydroxylases by bipyridinedicarboxylates, Bioorg. Med. Chem. 23 (2015) 3081–3090.
[24] J.D. Vasta, K.A. Andersen, K.M. Deck, C.P. Nizzi, R.S. Eisenstein, R.T. Raines, Selective inhibition of collagen prolyl 4-hydroxylase in human cells, ACS Chem. Biol. 11 (2016) 193–199.
[25] H.S. Chong, Y. Chen, C.S. Kang, X. Sun, N. Wu, Novel (64)Cu-radiolabeled bile acid conjugates for targeted PET imaging, Bioorg. Med. Chem. Lett. 25 (2015) 1082–1085.
[26] P.L. Anelli, L. Lattuada, V. Lorusso, G. Lux, A. Morisetti, P. Morosini, M. Serleti, F. Uggeri, Conjugates of gadolinium complexes to bile acids as hepatocyte-directed contrast agents for magnetic resonance Imaging, J. Med. Chem. 47 (2004) 3629–3641.
[27] E. Campazzi, M. Cattabriga, L. Marvelli, A. Marchi, R. Rossi, M.R. Pieragnoli, M. Fogagnolo, Organometallic radiopharmaceuticals: rhenium(I) carbonyl complexes of natural bile acids and derivatives, Inorg. Chim. Acta 286 (1999) 46–54.
[28] Z. Kejik, R. Kaplanek, M. Havlik, T. Briza, D. Vavrinova, B. Dolensky, P. Martasek, V. Kral, Aluminium(III) sensing by pyridoxal hydrazone utilising the chelation enhanced fluorescence effect, J. Lumin. 180 (2016) 269–277.
[29] M. Jakubek, Z. Kejík, V. Antonyová, R. Kaplánek, D. Sýkora, R. Hromádka, K. Vyhlídalová, P. Martásek, V. Král, Benzoisothiazole-1,1-dioxide-based synthetic receptor for zinc ion recognition in aqueous medium and its interaction with nucleic acids, Supramol. Chem. 31 (2019) 19–27.
[30] D.S. Kalinowski, D.R. Richardson, Future of toxicology-iron chelators and differing modes of action and toxicity: The changing face of iron chelation therapy, Chem. Res. Toxicol. 20 (2007) 715–720.
[31] G. Sridharan, R. Pratibha, P. Sangeeta, R. Vijayaraghavan, Analysis of estrogen metabolites in oral leukoplakia and oral squamous cell carcinoma, Int. J. Pharma Biol. Sci. 8 (2017) 5.
[32] F. Brito, N. Ingri, L.G. Sillen, Are aqueous metavanadate species trinuclear tetranuclear or both - preliminary letagrop recalculation of Emf data, Acta Chem. Scand. 18 (1964) 1557–1558.